Conformational Transition in SPR Experiments: Impact of spacer length, immobilization mode and aptamer density on signal sign and amplitude

M. Pons,[1] M. Perenon,[1] H. Bonnet,[1] E. Gillon,[2] C. Vallée,[1] L. Coche-Guérente,[1] E. Defrancq,[1] N. Spinelli,[1] A. Van der Heyden,[1*] J. Dejeu[1*]

1. Univ. Grenoble Alpes, CNRS, DCM UMR-5250, F-38000 Grenoble, France
2. Univ. Grenoble Alpes, CERMAV-CNRS, 601 rue de la chimie, F- 38610 Gières

Corresponding author: Jérôme Dejeu, + 33 (0)4 56 52 08 13, jerome.dejeu@univ-grenoble-alpes.fr ; Angéline Van der Heyden, +33 (0)4 56 52 08 14, angeline.van-der-heyden@univ-grenoble-alpes.fr

Determination of the refractive index increment (RII) of the aptamer in solution by SPR 2
Expression of the Jung equation 4
Expression of the Wilson Formula 5
Raw SPR signals recorded during L-Tym injection on the Apt_{23}-T_0-Biot and reference flow cells 6
SPR signals recorded during D-Tym injection on the Apt_{23}-T_0-Biot surface 7
Circular dichroism of the different Apt_{23}-T_x-Biot alone and in presence of L-Tym 8
Apparent Thermodynamic equilibrium constant for L-Tym/Apt_{23}-T_0-Biot interaction determined by QCM-D 9
ITC experiments for L-Tym recognition by Apt_{23} bearing various spacers 10
SPR signals recorded on active flow-cells exhibiting different Apt_{23}-T_0-Biot surface densities 12
Kinetic constants for Apt_{23}-T_0-Biot upon interaction with L-Tym 13
QCM-D signal recorded upon L-Tym injection on biotinylated Apt_{23} layers with different spacers 14
SPR signal recorded on Apt_{23}-A_6-Biot surface upon L-Tym injections 18
Raw SPR signal recorded on Apt_{23}-T_6-Biot and on reference flow cell upon L-Tym injections 18
Refractive Index Increment correction in the model developed by Dejeu et al 19
Comparison of experimental and expected maximal SPR signal for Apt_{23}-T_0-Biot upon interaction with L-Tym 20
Comparison of experimental and expected maximal SPR signal for Apt_{23}-T_6-Biot upon interaction with L-Tym 21

Determination of the refractive index increment (RII) of the aptamer in solution by SPR alone and in presence of *L*-Tym.

Briefly, injection of different concentrations of each aptamer were performed on a gold surface protected by a self-assembled monolayer (SAM) of HS-$(CH_2)_{11}$-EG_4–OH.

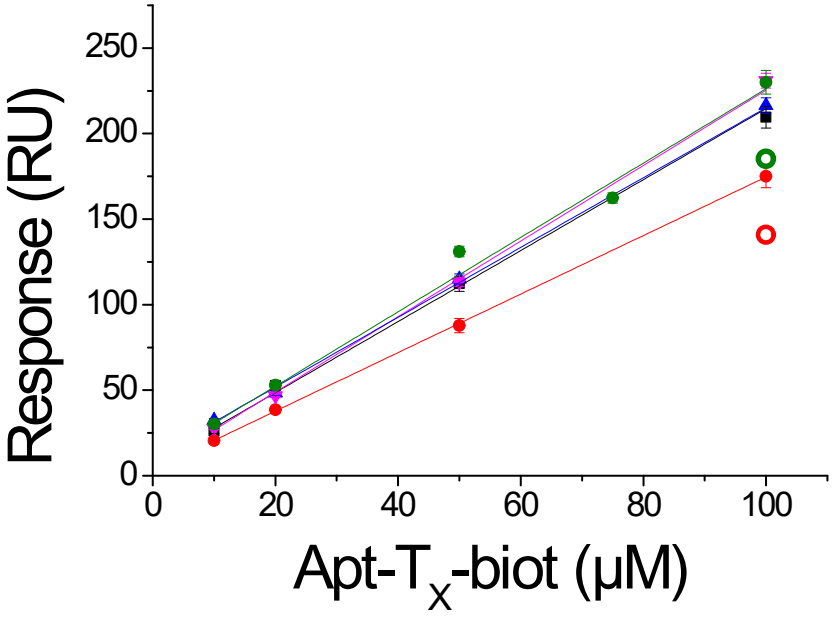

Figure SI-1. Variation of the recorded SPR equilibrium response versus the aptamer concentration in the running buffer (full point) and in presence of L-Tym 200µM (open circle): Apt_{23}-T_0-Biot (black), Apt_{23}-T_3-Biot (red), Apt_{23}-T_9-Biot (blue), Apt_{23}-T_{12}-Biot (pink) and Apt_{23}-A_6 (green). For Apt_{23}-A_6, the RII value was measured using the aptamer without the biotin function.

Figure SI- 1 represents the variation of the SPR responses recorded at equilibrium upon injection of aptamers at various concentration on the flowcell. The linearity of the response suggested that the aptamer does not adsorb on the surface, confirming the protective role of the pegylated SAM against non-specific adsorption. This observation was also supported by the square shape of the SPR signal upon injection (data don't show).The slope of the SPR response

variation versus the aptamer concentration allows the determination of it refractive index increment RII[1] based on the following equation:

$$RII_A = \frac{S.10^{-6}.10^3}{MW_A}$$ Equation SI- 1

Where S is the slope of the variation of the SPR response in function of the analyte concentration (expressed in RU. mol^{-1}.L), 10^{-6} term converts the RU value into Refractive Index Unit (RIU) according to 1 RU = 10^{-6} RIU (also equal to a shift of 10^{-4} degree of the resonance angle), 10^3 term converts litter to cm^3.

Expression of the Jung equation

The areal molar density of the aptamer (Γ_L^0) is function of the SPR signal recorded during the aptamer immobilization (RU_L) and is defined by Jung's equation[2] (Equation SI-2):

$$\Gamma_L^0 = RU_L \frac{1}{\left(\frac{dn}{dc}\right)_L} d_L \frac{1}{\left(e^{-\frac{d_0}{d_p}} - e^{-\frac{d_0+d_L}{d_p}}\right)}$$ Equation SI- 2

With $(dn/dc)_L$ the molar refractive index increment (RII) of the Apt_{23}-T_0-Biot, 1947.5 $cm^3.mol^{-1}$ determined in this study by SPR (See Table 1), d_0 the thickness of the layer composed of the biotinylated SAM and streptavidin, d_L the thickness of the aptamer layer and dp, the effective penetration depth of the evanescent wave (175 nm).[3-4] d_L was taken to 5.2 nm as previously discussed.[5]

Expression of the Wilson Formula

The SPR signal could be predicted according to the following formula introduced by Wilson.[6]

$$R_{A_{\max}} = RU_L \frac{MW_A.(dn/dc)'_A}{MW_L.(dn/dc)'_L} \times V = \beta.RU_L \times V \qquad \text{Equation SI- 3}$$

Where R_{Amax} is the predicted maximum response, RU_L is the amount of aptamer immobilized (500 RU), MW_A and MW_L are respectively the molecular weight of the analyte (*L*-Tym, 180.2 g.mol^{-1}) and of the immobilized aptamer, $(dn/dc)'_A$ and $(dn/dc)'_L$ are the mass refractive index increments (RII) for *L*-Tym (0.219 cm^3.g^{-1})[5] and for the aptamer (see Table 1 in the manuscript) respectively. $\beta = MW_A.(dn/dc)'_A / MW_L.(dn/dc)'_L$ is the ratio of the mass-weighted RII of the analyte *versus* the ligand (*i.e.* the ratio of the molar RII) and *V*, the *Valency i.e.* the ratio number of analytes *per* number of ligands involved in the recognition (*V*=1 in the present system[7]).

Raw SPR signals recorded during L-Tym injection on the Apt_{23}-T_0-Biot and reference flow cells

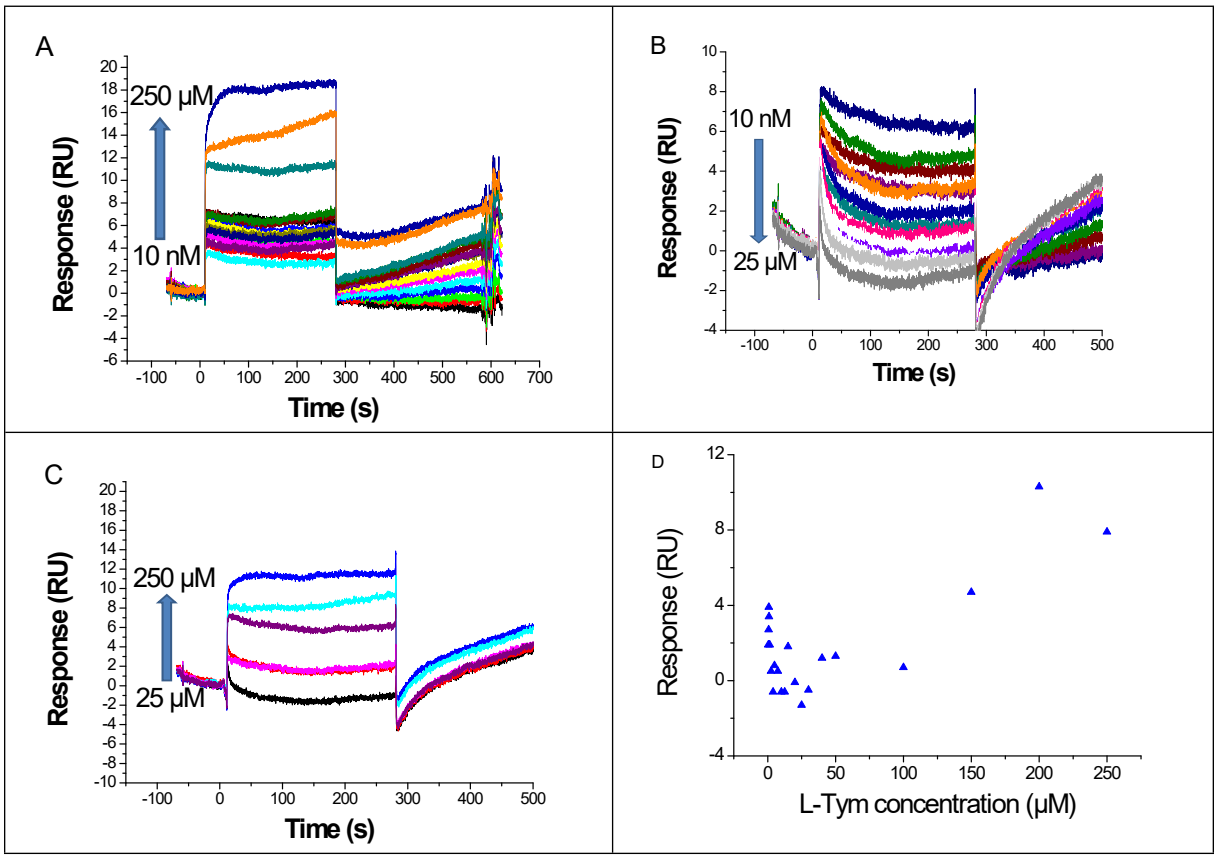

Figure SI-2. SPR curves recorded during the injections of L-Tym on A) the reference flow-cell (biotinylated random DNA sequence) with L-Tym for concentrations ranging from 10 nM to 250 µM B) Apt_{23}-T_0-Biot surface at low L-Tym concentration (below 25µM), C) Apt_{23}-T_0-Biot at high L-Tym concentration (above 25 µM). D) SPR signal intensity during the interaction of L-Tym with Apt_{23}-T_0-Biot.T= 25°C. Flow rate: 30µL/min. 480 RU of was Apt_{23}-T_0- Biot immobilized.

SPR signals recorded during D-Tym injection on the Apt_{23}-T_0-Biot surface

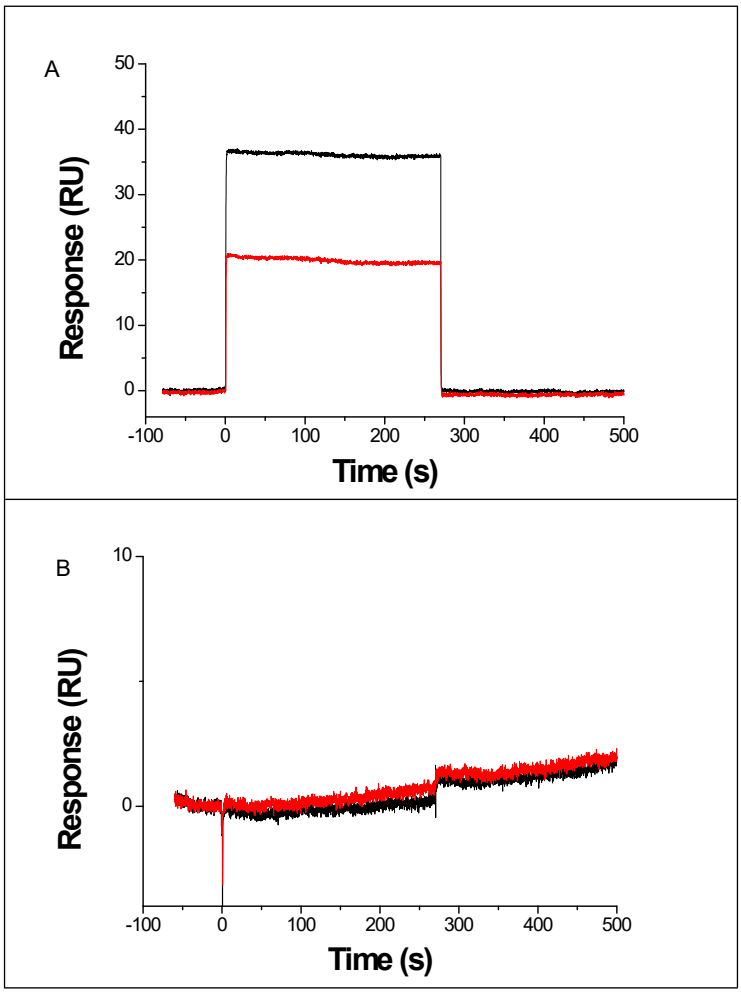

Figure SI-3. Figure SPR curves recorded during the injections of D-Tym at concentration 100 µM (red) and 1 mM (black) on Apt_{23}-T_0-Biot surface A) before and B) after double-reference-subtraction procedure. Flow rate: 30µL/min. The immobilization signal for Apt_{23}-T_0- Biot was 480 RU.

Circular dichroism of the different Apt_{23}-T_x-Biot alone and in presence of L-Tym

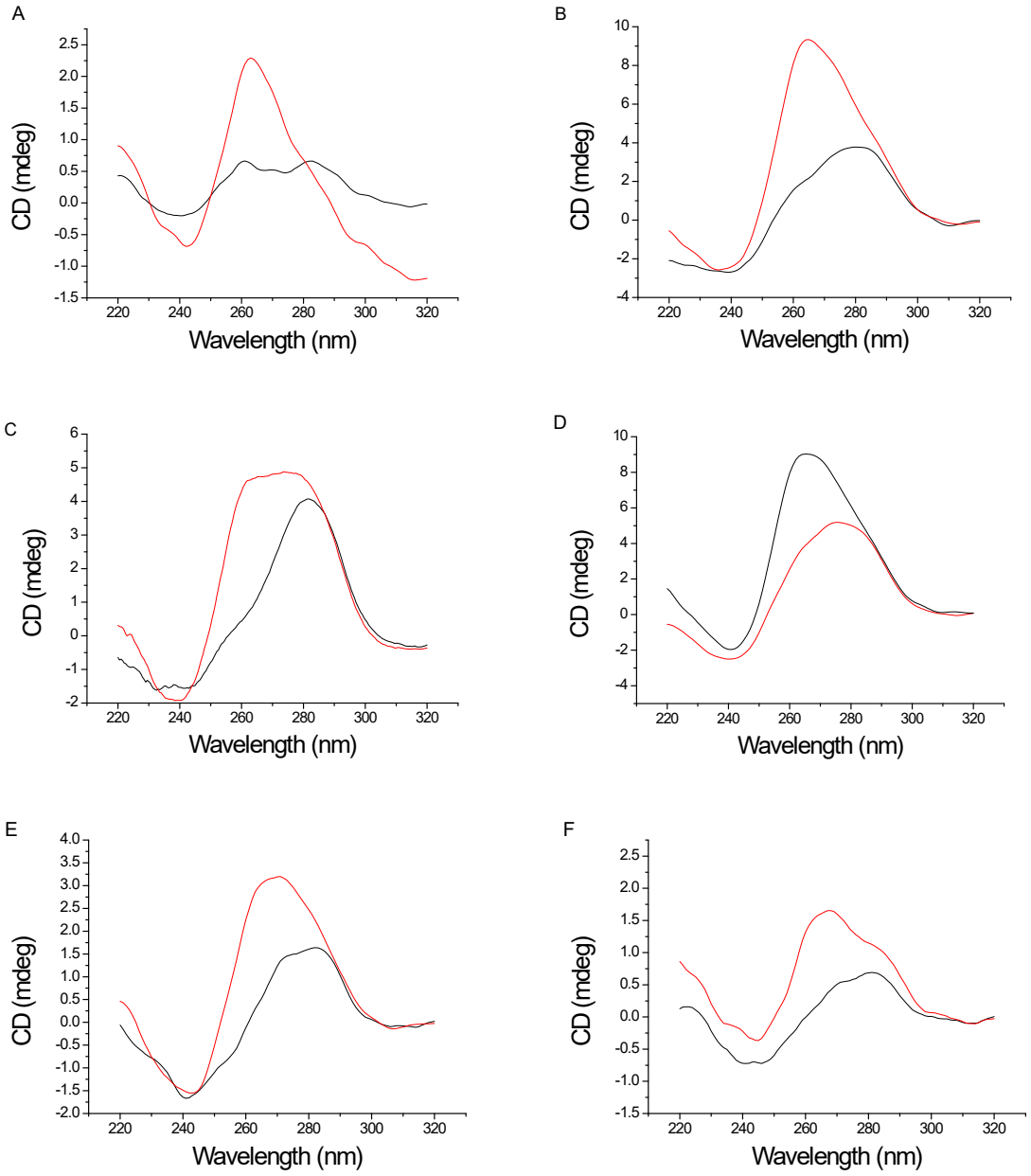

Figure SI-4. CD spectra of Apt_{23}-T_x-Biot alone (black) and in presence of L-Tym (red): A) Apt_{23}-T_0-Biot, B) Apt_{23}-T_3-Biot, C) Apt_{23}-T_6-Biot, D) Apt_{23}-A_6-Biot, E) Apt_{23}-T_9-Biot, F) Apt_{23}-T_{12}-Biot.

Apparent Thermodynamic equilibrium constant for L-Tym/Apt_{23}-T_0-Biot interaction determined by QCM-D

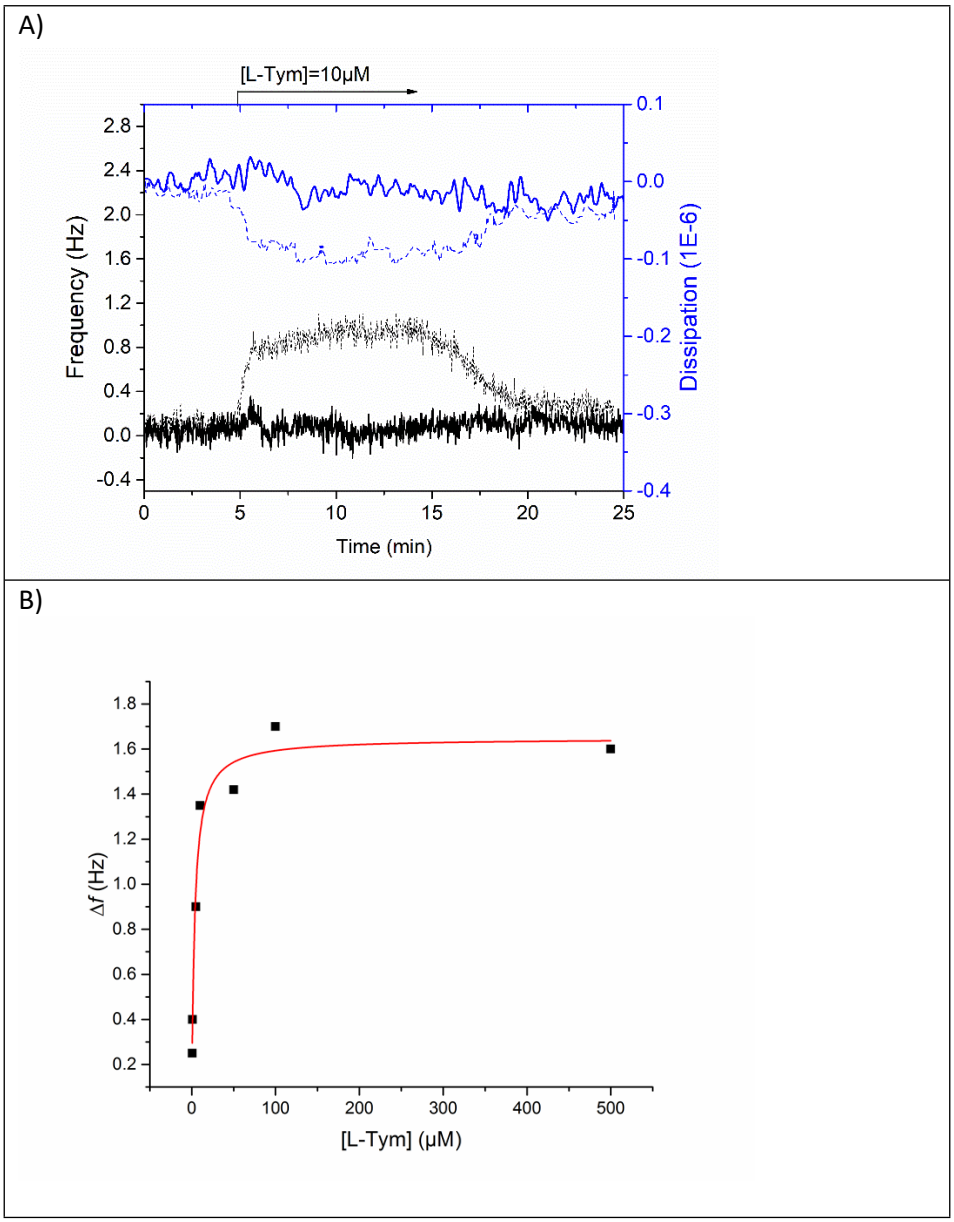

Figure SI-5. A) Variation of the frequency and dissipation shift recorded upon injection of L-Tym 10µM on Apt_{23}-T_6-Biot layer (thin dotted line) and on the scramble layer (thick solid line); B) Variation of the frequency shift for Apt_{23}-T_6-Biot as a function of L-Tym concentrations for the 7th overtone (black squares). Result of fitting (red line) to a 1:1 interaction model (Langmuir isotherm) leading to an average apparent equilibrium dissociation constant $K_{D,app}$ of 3.3± 0.9 µM. Note that this K_D values should be considered as an apparent K_D (noted $K_{D,app}$), as it was indirectly obtained from the quantification of the expelled water upon L-Tym binding and not to the added mass of L-Tym trapped by the aptamer layer.[4, 8]

ITC experiments for L-Tym recognition by Apt_{23} bearing various spacers

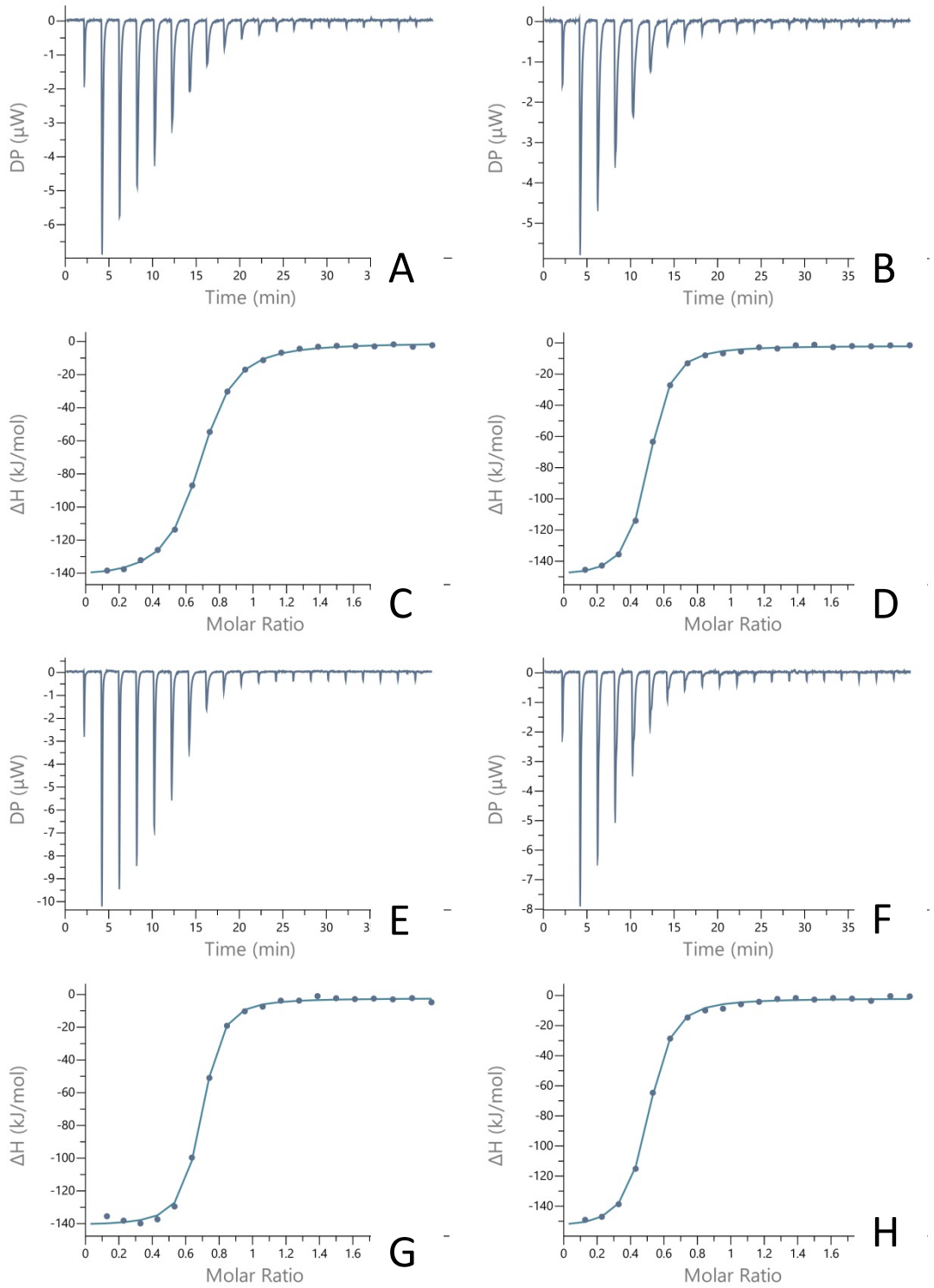

Figure SI-6. Isothermal titration calorimetry measurements at 25 °C for serial injections of 250 µM Apt_{23}-T_x in running buffer (10 mM Tris, 50 mM NaCl, 5 mM $MgCl_2$ pH 7.4) into the cell loaded with the L-Tym at concentrations of 25 µM: **A** and **C** Apt_{23}-T_0, **B** and **D** Apt_{23}-T_3, **E** and **G** Apt_{23}-T_6, and **F** and **H** Apt_{23}-A_6. **A**, **B**, **E** and **F**: Baseline-corrected titration curve (apart for the first one, the injections were of 2 µL). **C**, **D**, **G** and **H**: fit of the integrated titration curve with Microcal PEAQ-ITC analysis software.

Table SI-1. Thermodynamic parameters determined by ITC for the recognition of the L-Tym by the MBS bearing various spacers

	Apt_{23}-T_0	Apt_{23}-T_3	Apt_{23}-T_6	Apt_{23}-A_6
K_D (μM)	0.42 ± 0.02	0.23 ± 0.02	0.13 ± 0.01	0.27 ± 0.02
ΔH (kJ.mol^{-1})	–137 ± 5	–149 ± 1	–139 ± 0	–154 ± 1
T.ΔS (kJ.mol^{-1})	–101 ± 5	–111 ± 1	–100 ± 1	–117 ± 1

SPR signals recorded on active flow-cells exhibiting different Apt_{23}-T_0-Biot surface densities

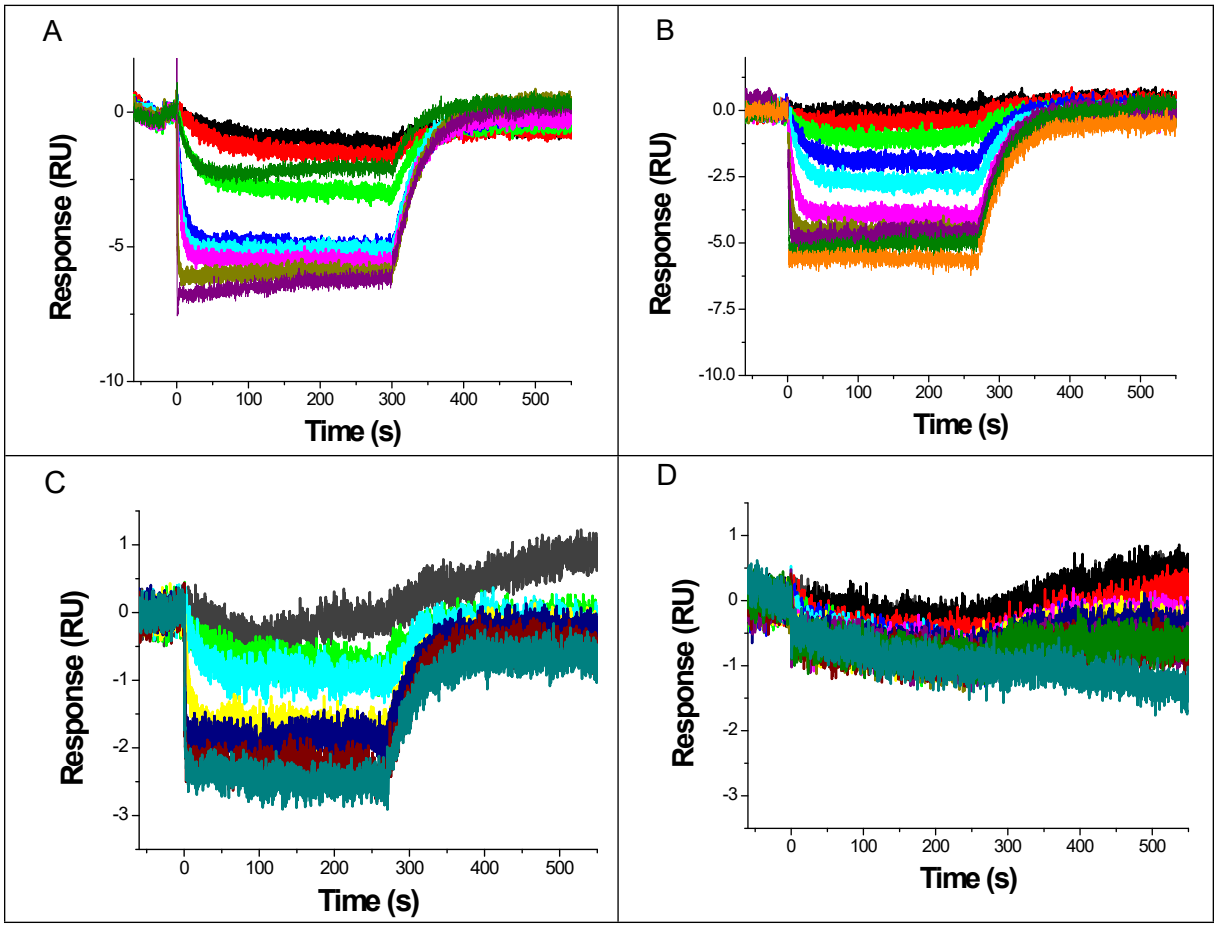

Figure SI-7. Sensorgrams recorded during injection of L-Tym (from 10 nM to 50 µM) after double-reference-subtraction procedure for a immobilization signal for Apt_{23}-T_0-Biot of: A) 421 RU, B) 269 RU, C) 179 RU, D) 60 RU. T = 25 °C. Flow rate: 30 µL min^{-1}.

Kinetic constants for Apt_{23}-T_0-Biot upon interaction with L-Tym

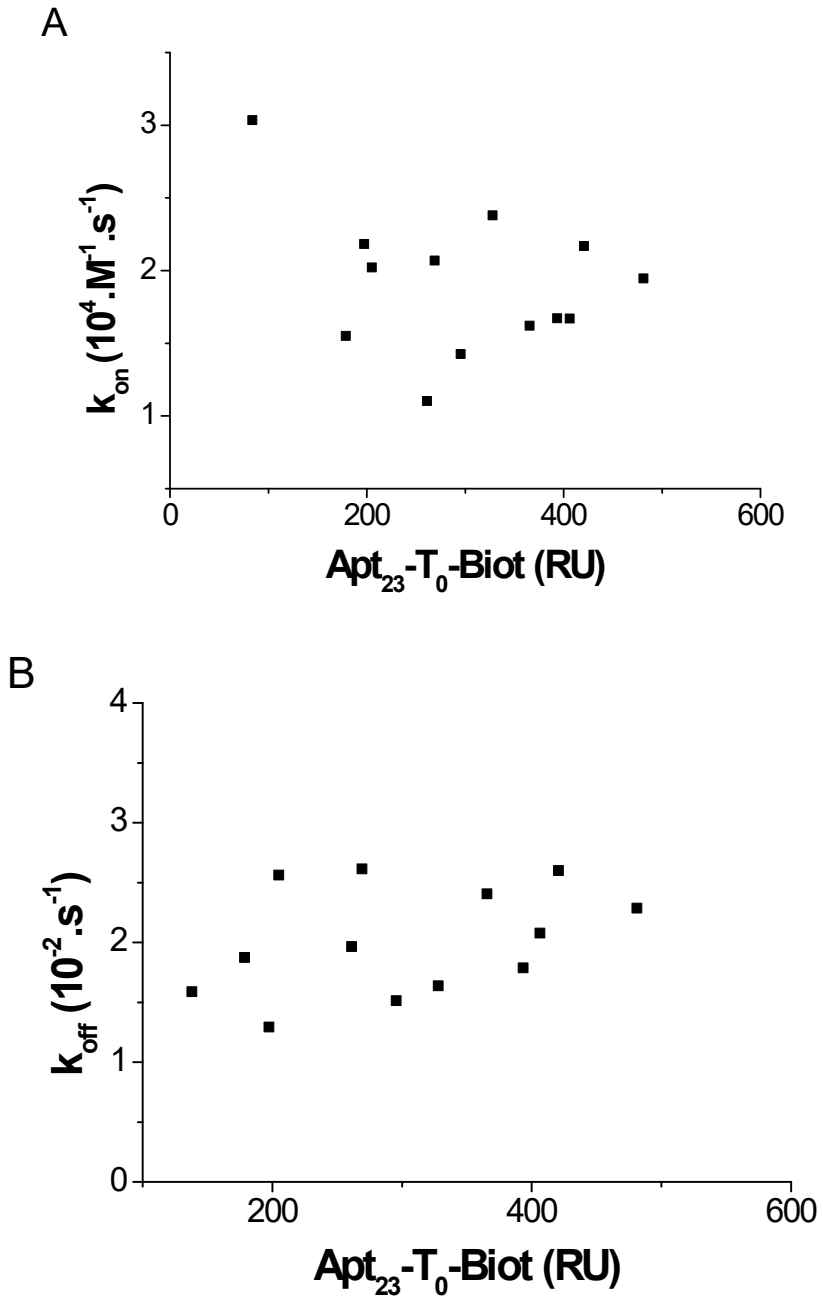

Figure SI-8. Variation of the kinetic parameters of the interaction determined by SPR as a function of Apt_{23}-T_0-Biot density on the sensing layer A) variation of the association kinetic constant k_{on}, B) variation of the dissociation kinetic constant k_{off}.

QCM-D signal recorded upon L-Tym injection on biotinylated Apt_{23} layers with different spacers

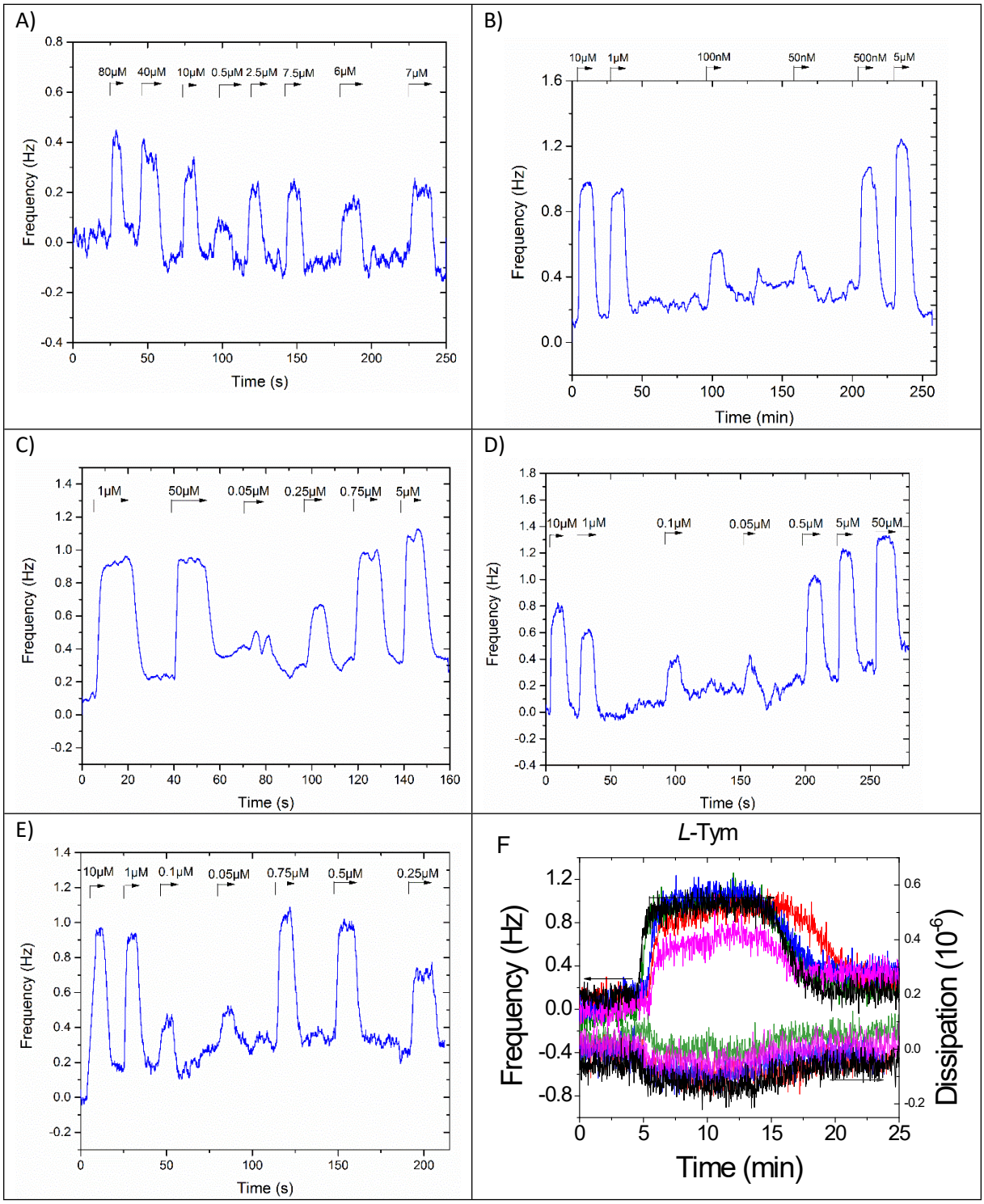

Figure SI-9. QCM-D signals (i = 7), after smoothing, recorded during the exposure of L-Tym solution (at concentrations between 0.05 and 10 μM) A) Apt_{23}-T_3-Biot, B) Apt_{23}-T_6-Biot, C) Apt_{23}-A_6-Biot, D) Apt_{23}-T_9-Biot and E) Apt_{23}-T_{12}-Biot functionalized transducer surface. F) QCM-D signals (i = 7) recorded during the exposure of L-Tym solution at 10 μM to a Apt_{23}-T_3-Biot (pink), Apt_{23}-T_6-Biot (black), Apt_{23}-A_6-Biot (green), Apt_{23}-T_9-Biot (red) and Apt_{23}-T_{12}-Biot (blue) functionalized transducer surface.

The results summarized in the table SI-2 were the average and the standard deviation of at least two independent experiments: different surfaces, different aptamer aliquots and different concentration of L-Tym solution.

Table SI-2: Apparent affinity constant (K_{Dapp}) determined by the fitting of the QCM-D data with a Langmuir isotherm for the different aptamers studied.

Ligand	Apt_{23}-T_0-Biot	Apt_{23}-T_3-Biot	Apt_{23}-T_6-Biot	Apt_{23}-A_6-Biot	Apt_{23}-T_9-Biot	Apt_{23}-T_{12}-Biot
K_{Dapp} (μM)	3.3 ± 0.9	0.7 ± 0.3	0.2 ± 0.1	0.2± 0.1	0.2 ± 0.1	0.2 ± 0.1

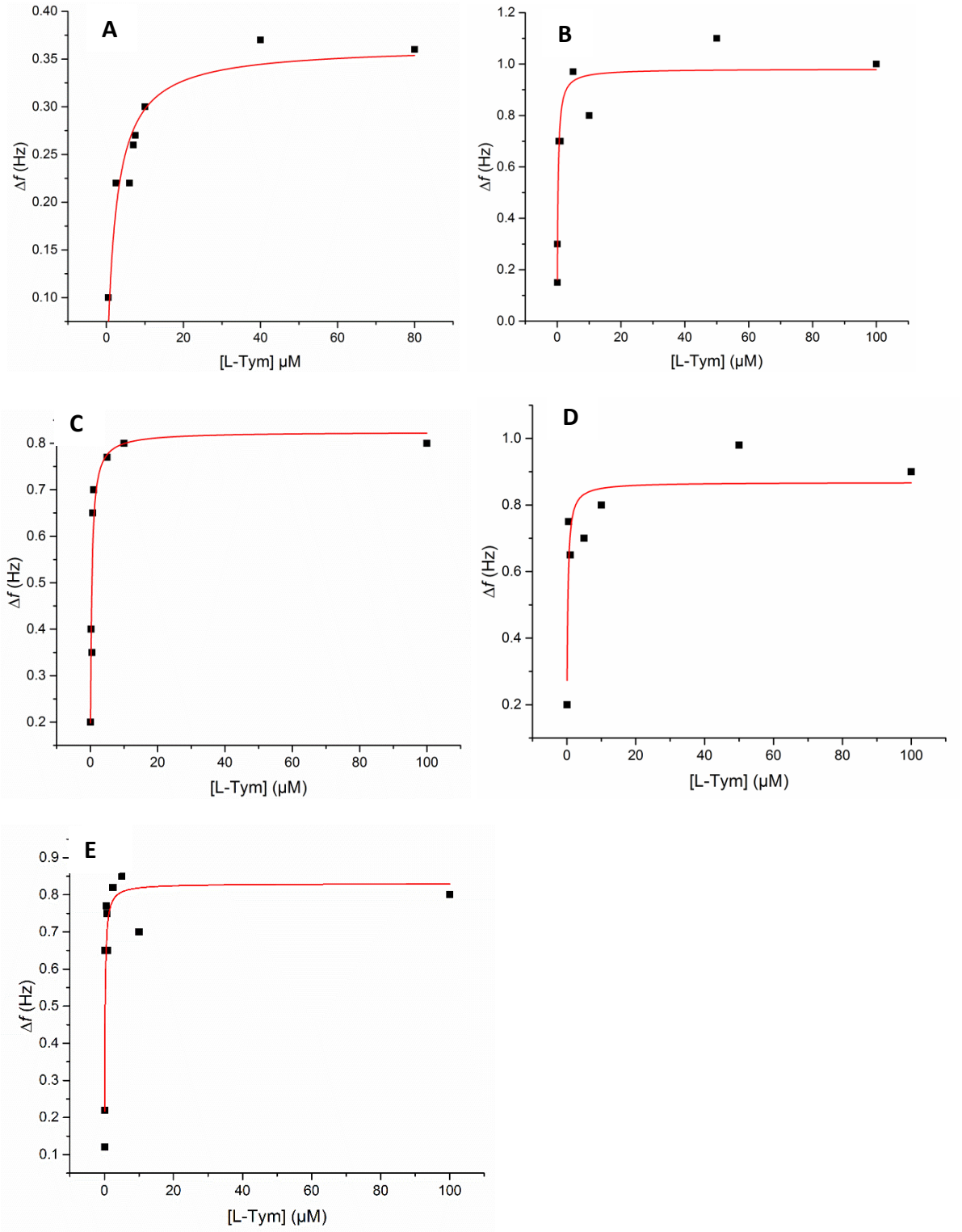

Figure SI-10. Variation of the resonance frequency as a function of L-Tym concentrations for the 7th overtone (black square) and fitted (red line) to a 1:1 binding curve (Langmuir isotherm) for A) Apt_{23}-T_3-Biot, B) Apt_{23}-T_6-Biot, C) Apt_{23}-A_6-Biot, D) Apt_{23}-T_9-Biot and E) Apt_{23}-T_{12}-Biot.

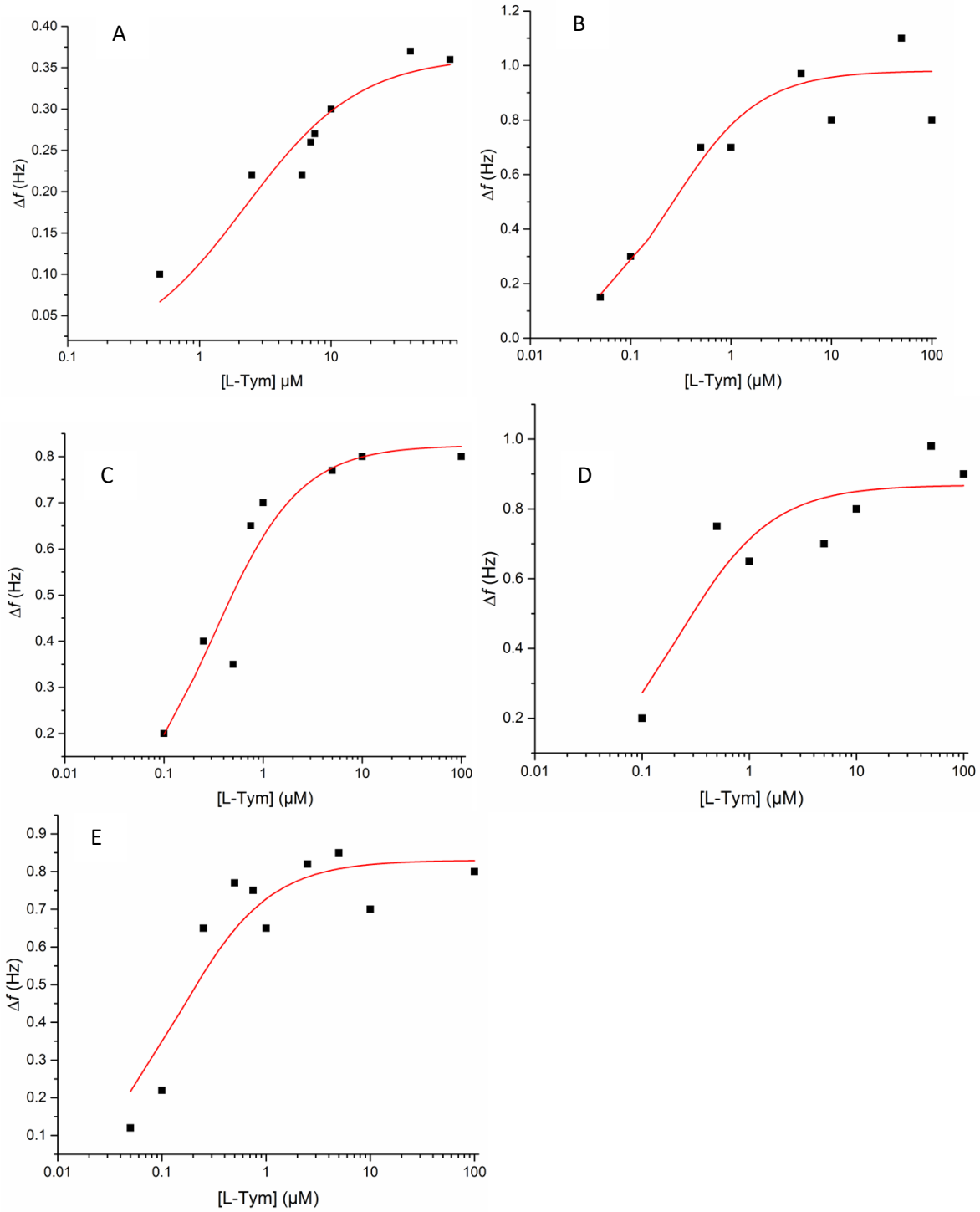

Figure SI-11. Variation of the resonance frequency as a function of L-Tym concentrations for the 7th overtone (black square) and fitted (red line) to a 1:1 binding curve (Langmuir isotherm) with a logarithm x axis for A) Apt_{23}-T_3-Biot, B) Apt_{23}-T_6-Biot, C) Apt_{23}-A_6-Biot, D) Apt_{23}-T_9-Biot and E) Apt_{23}-T_{12}-Biot.

SPR signal recorded on Apt_{23}-A_6-Biot surface upon L-Tym injections

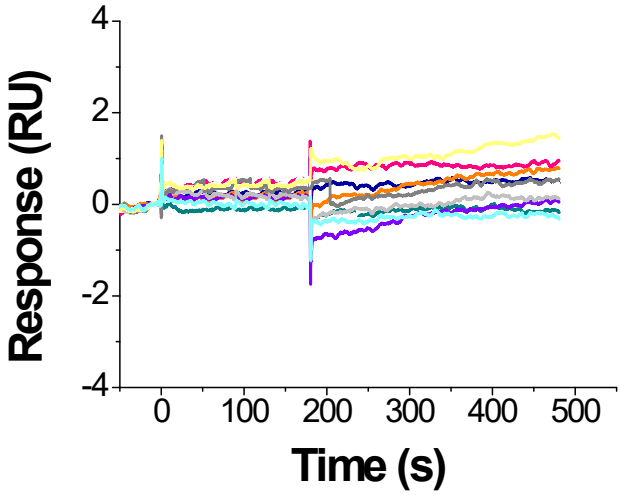

Figure SI-12. SPR curves recorded upon injection of L-Tym solution at concentrations ranging from 10 nM to 250 µM on Apt_{23}-A_6-Biot. T= 25°C. Flow rate: 30 µL/min.

Raw SPR signal recorded on Apt_{23}-T_6-Biot and on reference flow cell upon L-Tym injections

The signal was similar whatever the Apt_{23}-T_X-Biot (X>1) immobilized.

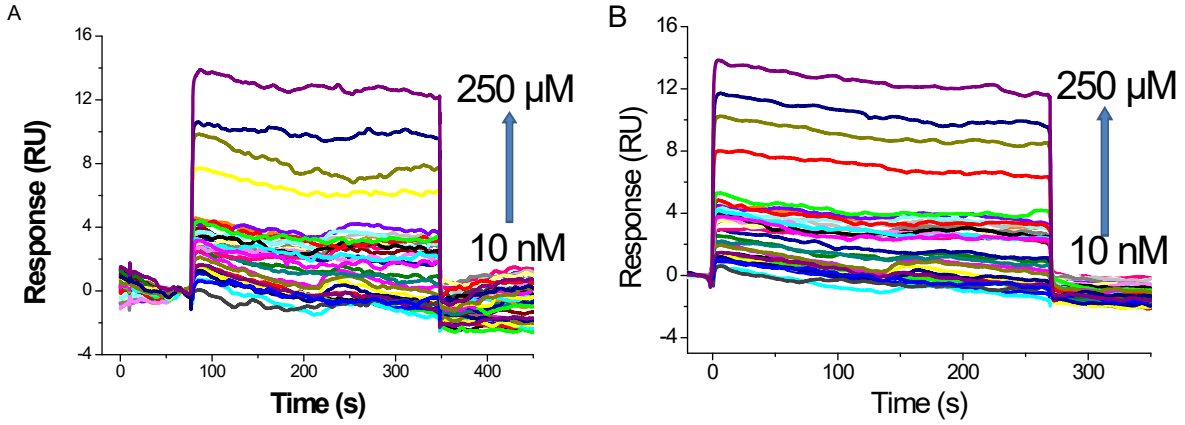

Figure SI-13. SPR curves recorded upon injection of L-Tym solution at concentrations ranging from 10 nM to 250 µM on A) the reference flow-cell (biotinylated scramble) and B) Apt_{23}-T_6-biot. T= 25°C. Flow rate: 30 µL/min

Refractive Index Increment correction in the model developed by Dejeu et al

See the article of Dejeu et al[5] for further details.

Classically, the molar refractive index increment of the complex analyte/ligand can be defined from the RII of both the analyte and the ligand ones by equation SI- 4:

$$\left(\frac{dn}{dc}\right)_{LA} = \left(\frac{dn}{dc}\right)_{L} + V.\left(\frac{dn}{dc}\right)_{A} \qquad \text{Equation SI- 4}$$

The L-Tym/aptamer interaction having a 1:1 stoichiometry,[3] V=1 in our study

Considering a deviation factor for the RII of the analyte/ligand complex, equation SI- 4 is not valid anymore and a correction term has to be included. As a consequence, the RII of the L-Tym/aptamer complex is expressed as a function of the RII of the aptamer by introducing a correction factor, x:

$$\left(\frac{dn}{dc}\right)_{correction} = x\left(\frac{dn}{dc}\right)_{L} \qquad \text{Equation SI- 5}$$

where $(dn/dc)_{correction}$ is the correction of the L-Tym/aptamer complex RII defined as a function of the RII of the aptamer. By adding this correction factor to the sum of the RII of the two entities separately considered equation SI- 4, we obtain equation SI-6:

$$\left(\frac{dn}{dc}\right)_{LA} = \left(\frac{dn}{dc}\right)_{L} + V.\left(\frac{dn}{dc}\right)_{A} + \left(\frac{dn}{dc}\right)_{correction} = (1+x)\left(\frac{dn}{dc}\right)_{L} + V.\left(\frac{dn}{dc}\right)_{A} \qquad \text{Equation SI- 6}$$

Comparison of experimental and expected maximal SPR signal for Apt_{23}-T_0-Biot upon interaction with L-Tym

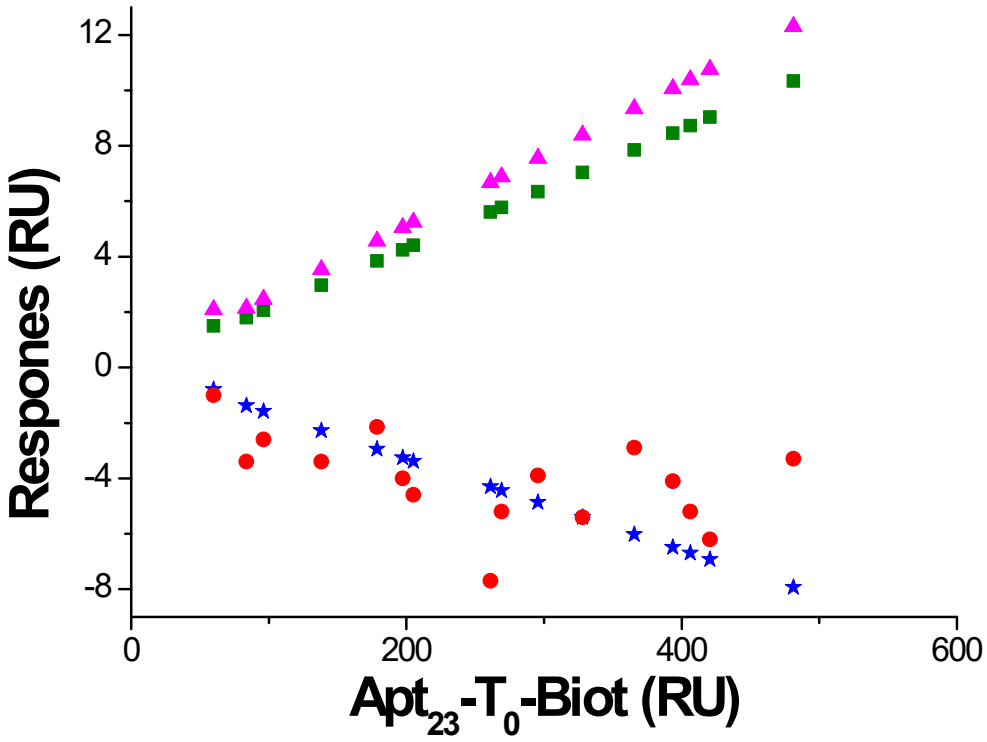

Figure SI-14. Comparison of the maximal response experimentally measured (red circle) for the interaction between L-Tym with Apt_{23}-T_0-Biot surface, expected from the Wilson's equation[6] (green square) and expected from Dejeu's equation[3] with folding of the aptamer and with (blue star) or without (pink triangle) RII deviation. Calculation were made with d_p=175nm, d_L=5.2 nm,[5] ρ=0.73,[5] β= 0.0307 (see Table 1 of the manuscript) and x= –0.0424.

Comparison of experimental and expected maximal SPR signal for Apt_{23}-T_6-Biot upon interaction with L-Tym

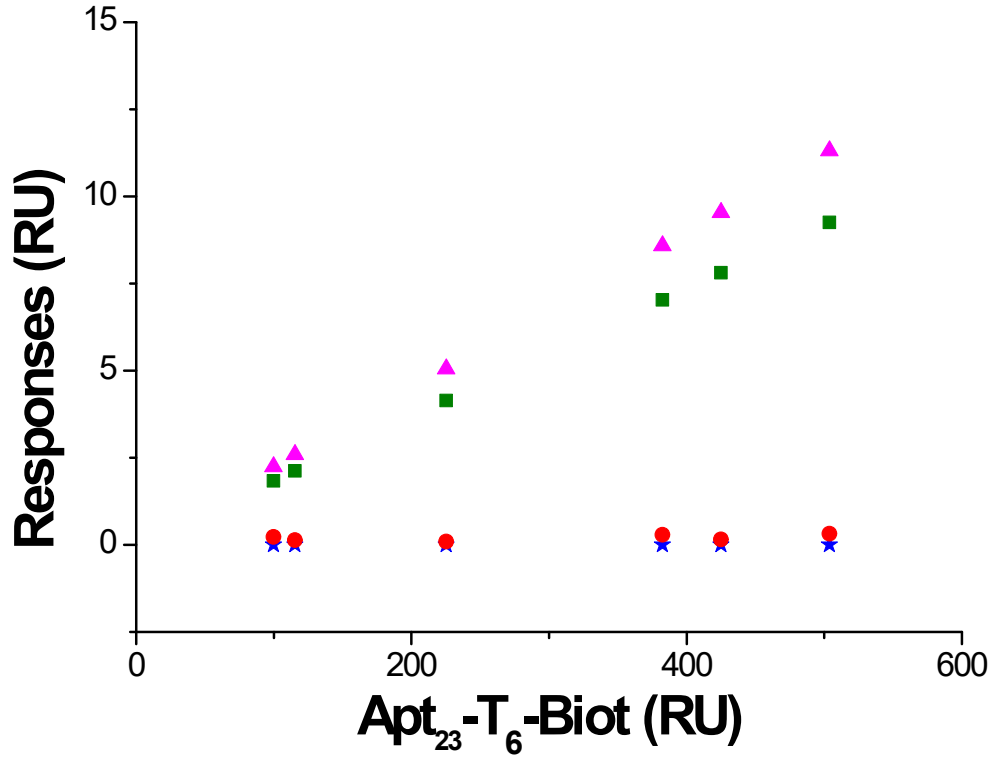

Figure SI-15. Comparison of the maximal SPR response experimentally measured (red circle) for the interaction between L-Tym with Apt_{23}-T_6-Biot surface, expected from the Wilson's equation[6] (green square) and expected from Dejeu's equation[3] with folding of the aptamer and with (blue star) or without RII variation (pink triangle). Calculation were made with d_p=175nm, d_L=5.2 nm, [5] ρ=0.73, [5] β= 0.0184 (See Table 1 of the manuscript) and x=-0.0198.

References

1. Tumolo, T.; Angnes, L.; Baptista, M. S., Determination of the Refractive Index Increment (dn/dc) of Molecule and Macromolecule Solutions by Surface Plasmon Resonance. *Anal. Biochem.* **2004,** *333* (2), 273-279.

2. Jung, L. S.; Campbell, C. T.; Chinowsky, T. M.; Mar, M. N.; Yee, S. S., Quantitative Interpretation of the Response of Surface Plasmon Resonance Sensors to Adsorbed Films. *Langmuir* **1998,** *14* (19), 5636-5648.

3. Dejeu, J.; Bonnet, H.; Spinelli, N.; Defrancq, E.; Coche-Guérente, L.; Van der Heyden, A.; Labbé, P., Impact of Conformational Transitions on SPR Signals—Theoretical Treatment and Application in Small Analytes/Aptamer Recognition. *J. Phys. Chem. C* **2018,** *122* (37), 21521-21530.

4. Osypova, A.; Thakar, D.; Dejeu, J.; Bonnet, H.; Van der Heyden, A.; Dubacheva, G. V.; Richter, R. P.; Defrancq, E.; Spinelli, N.; Coche-Guérente, L.; Labbé, P., Sensor Based on Aptamer Folding to Detect Low-Molecular Weight Analytes. *Anal. Chem.* **2015,** *87* (15), 7566-7574.

5. Bonnet, H.; Coche-Guérente, L.; Defrancq, E.; Spinelli, N.; Van der Heyden, A.; Dejeu, J., Negative SPR Signals during Low Molecular Weight Analyte Recognition. *Anal. Chem.* **2021,** *93* (8), 4134-4140.

6. Davis, T. M.; Wilson, W. D., Determination of the Refractive Index Increments of Small Molecules for Correction of Surface Plasmon Resonance Data. *Anal. Biochem.* **2000,** *284* (2), 348-353.

7. Challier, L.; Miranda-Castro, R.; Barbe, B.; Fave, C.; Limoges, B.; Peyrin, E.; Ravelet, C.; Fiore, E.; Labbé, P.; Coche-Guérente, L.; Ennifar, E.; Bec, G.; Dumas, P.; Mavré, F.; Noël, V., Multianalytical Study of the Binding Between a Small Chiral Molecule and a DNA Aptamer: Evidence for Asymmetric Steric Effect upon 3′- versus 5′-End Sequence Modification. *Anal. Chem.* **2016,** *88* (23), 11963-11971.

8. MacDonald, H.; Bonnet, H.; Van der Heyden, A.; Defrancq, E.; Spinelli, N.; Coche-Guérente, L.; Dejeu, J., Influence of Aptamer Surface Coverage on Small Target Recognition: A SPR and QCM-D Comparative Study. *J. Phys. Chem. C* **2019,** *123* (22), 13561-13568.